
Supplementary materials

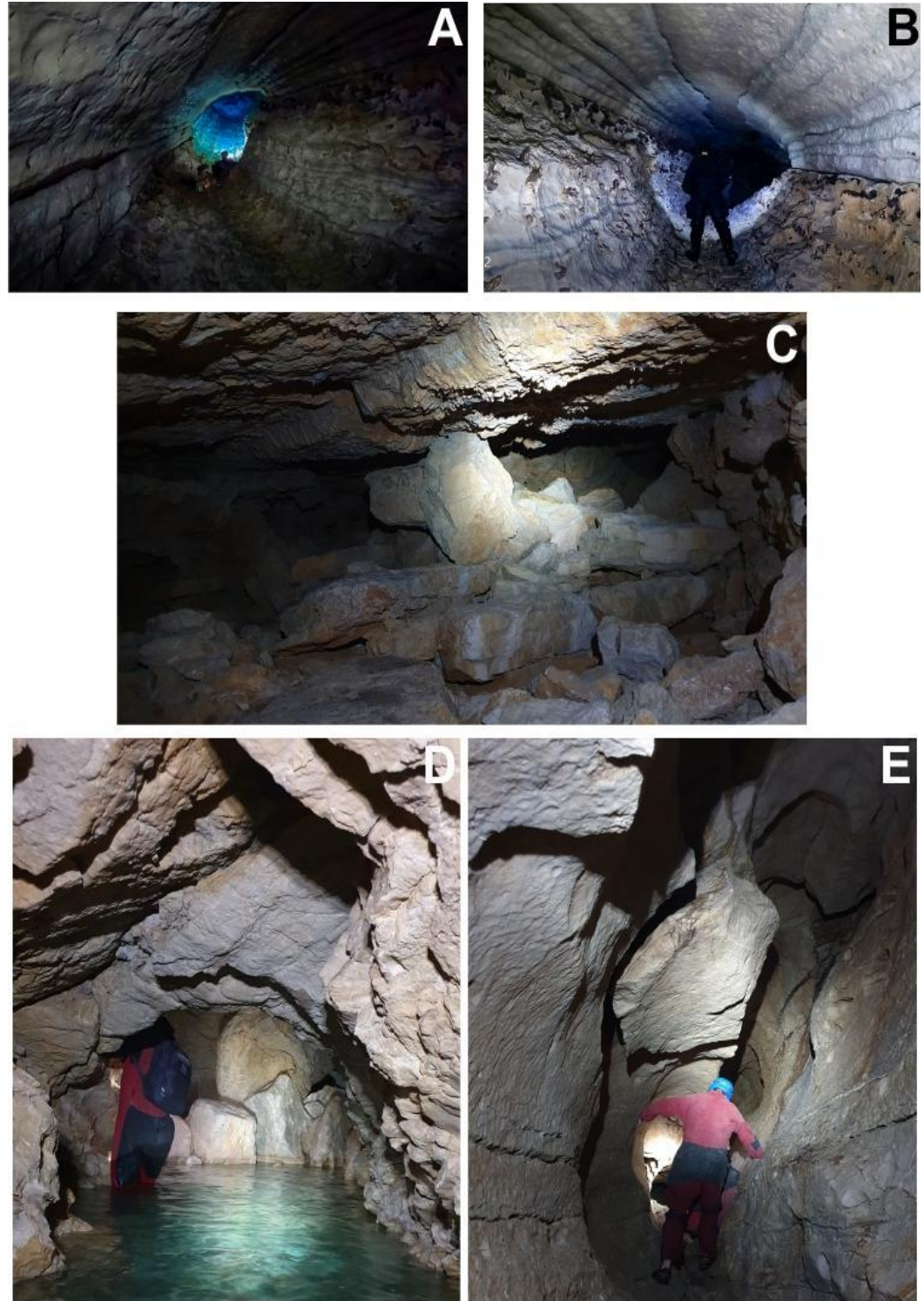


Figure S1. Karst Network of FA and Natividad springs. (A) Flooded conduit of Natividad spring. (B) Aerial conduit of Natividad spring. (C) Collapsed chamber in the FA karst network. (D) Karst gallery associated to FA. (E) Drainage conduit of FA spring.

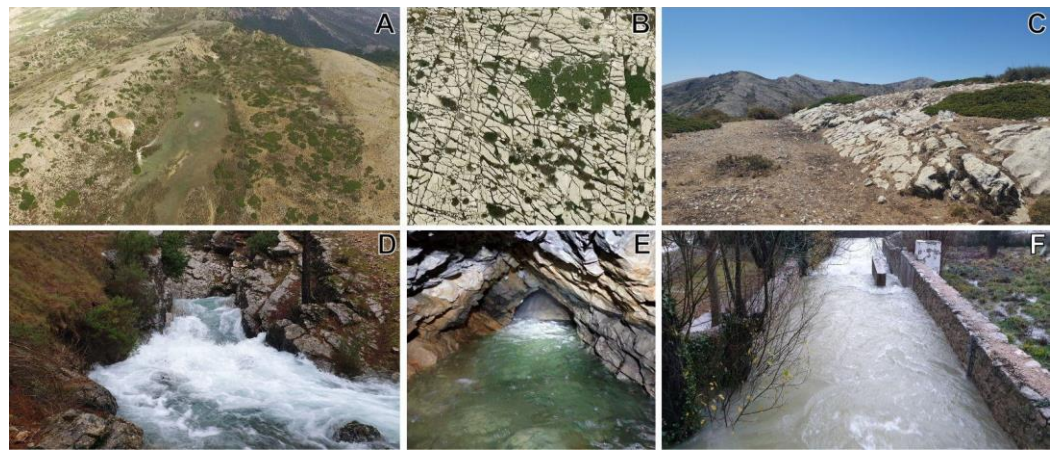


Figure S2. Kast development of study area. (A) Uvala "La Laguna" with ponor. (B) Lapiaz. (C) kastified surface. (D) Fuente Alta Spring. (E) Natividad Spring. (F) La Natividad Gauging station.



Figure S3. Activation sequence of the Fuente Alta Trop Pleins. (A) Trop Plein 1 inactive. (B) Trop Plein 1 active with low discharge flow rate (600 l/s). (C) Trop Plein 1 active with high discharge flow rate (4000 l/s). (D) Trop Plein 2 active. (E) Trop Plein 3 active. (F) Trop Plein 3 active.

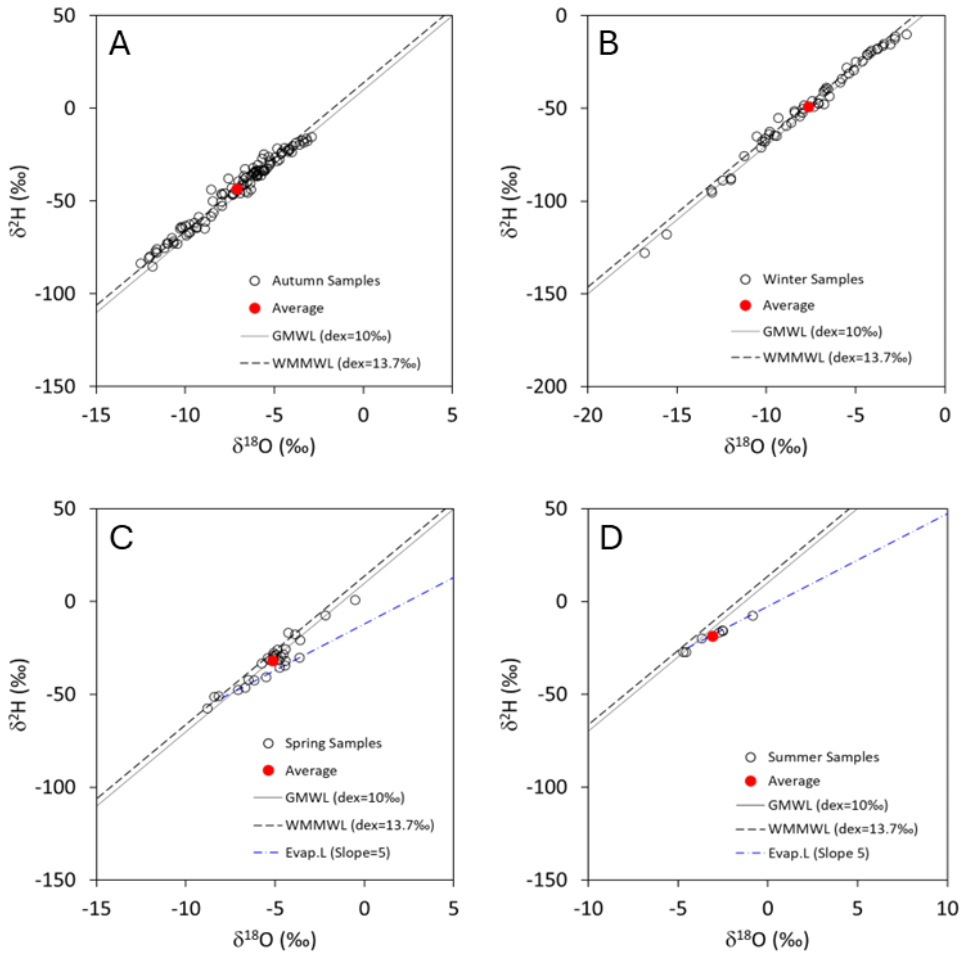


Figure S4. Seasonal variation of the isotopic content of precipitation. WMMWL, GMLW and Evap. L indicate West Mediterranean Meteoric Water Line (d -excess = 13.7 ‰), Global Meteoric Water Line (d -excess = 10 ‰), and Evaporation Line (slope $d\delta^2\text{H}/d\delta^{18}\text{O} = 5$), respectively. (A) Autumn. (B) Winter. (C) Spring. (D) Summer.

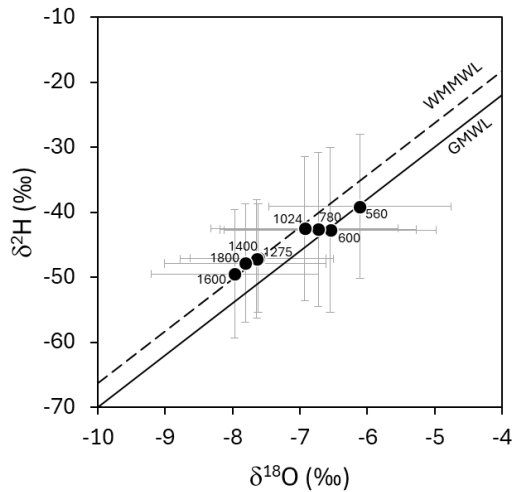


Figure S5. Mean isotopic content ($\delta^{18}\text{O}$) of precipitation in the rainfall monitoring stations. The numbers indicate the elevation of the rainfall monitoring stations. The two-sided error bars indicate one standard deviation. WMMWL and GMLW indicate West Mediterranean Meteoric Water Line (d -excess = 13.7 ‰), and Global Meteoric Water Line (d -excess = 10 ‰), respectively.

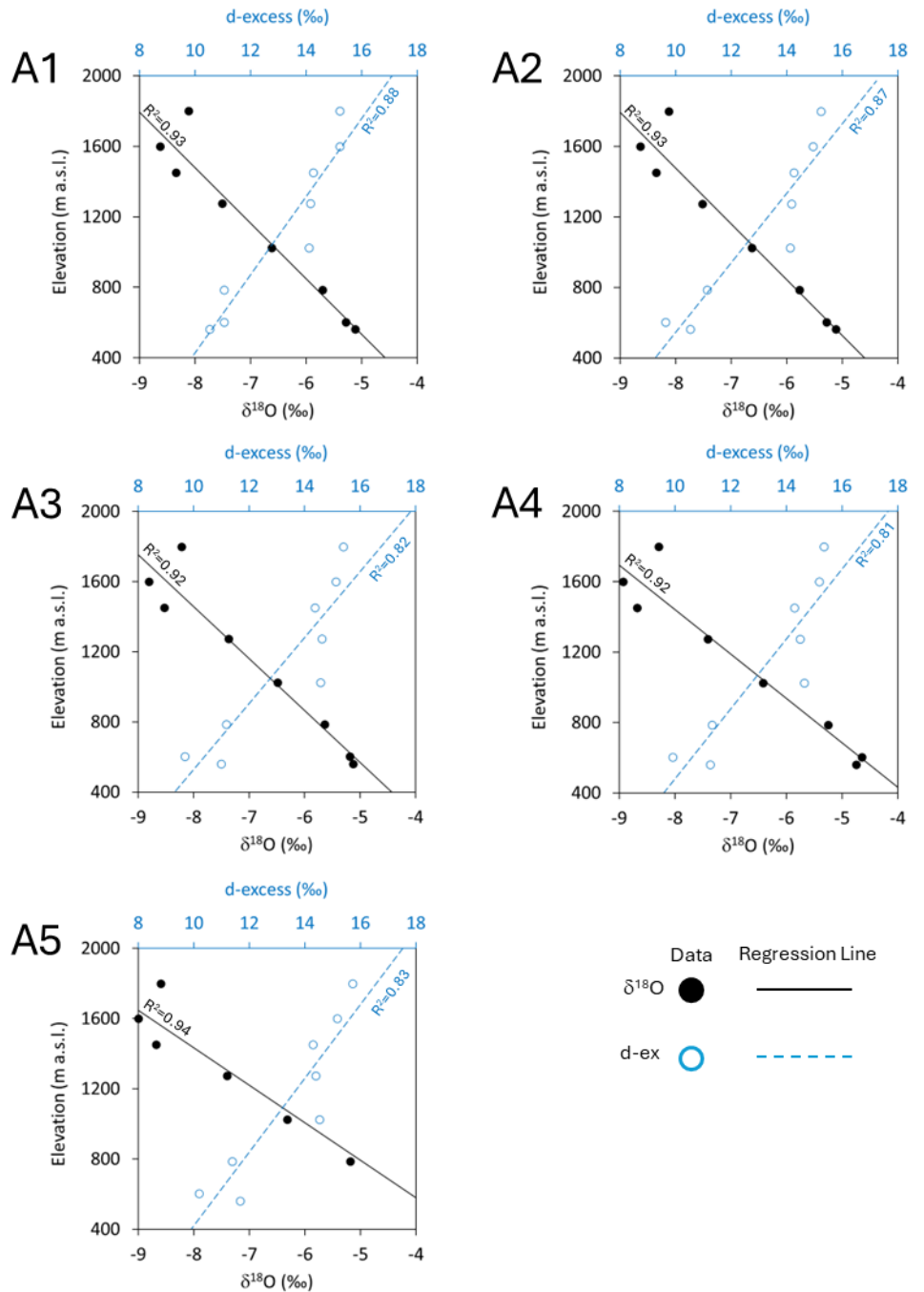


Figure S6. Isotopic ($\delta^{18}\text{O}$ and d-ex) Altitudinal Lines (IALs) of recharge for the different cases (i.e. A1 to A5) considered to estimate the mean isotopic content of recharge from that of precipitation.

Table S1. Mean isotopic content of precipitation at the sampling sites. Such isotope averages are obtained by excluding water samples from precipitation events of less than 20 mm.

Type	Sampling Point	Num. samples	Sampling period	Elevation (m a.s.l.)	$\delta^{18}\text{O}$ (‰)	$\delta^2\text{H}$ (‰)	d-ex (‰)
Precipitation	P. Génave	40	12/2017–09/2022	560	-6.11±2.70	-39.12±22.15	9.41±3.87
Precipitation	Lobo	33	01/2018–09/2022	600	-6.55±3.15	-42.73±25.26	9.36±3.04
Precipitation	R. Orcera	35	12/2017–09/2022	780	-6.73±2.92	-42.64±23.67	11.11±2.95
Precipitation	Dep. Segura	41	12/2017–09/2022	1024	-6.93±2.77	-42.49±22.15	12.23±2.77
Precipitation	Cortijo	59	12/2017–09/2022	1275	-7.62±2.01	-47.06±16.64	13.45±3.11
Precipitation	Yelmo 1400	40	05/2020–09/2022	1400	-7.64±2.27	-47.15±18.17	13.46±4.32
Precipitation	Yelmo 1600	29	10/2020–04/2022	1600	-7.97±2.48	-49.51±19.75	13.93±2.13
Precipitation	Yelmo 1800	30	12/2017–09/2022	1800	-7.81±2.39	-47.86±18.25	14.32±4.37
Groundwater	Enmedio	17	12/2020–10/2022	1080	-8.54±0.26	-56.34±1.69	12.01±0.74
Groundwater	Fuente Alta	22	10/2018–10/2022	1140	-8.73±0.41	-57.37±2.36	12.62±1.45
Groundwater	Natividad	28	10/2018–10/2022	1090	-8.69±0.34	-57.22±1.74	12.30±1.33

Table S2. Vertical isotopic gradient of precipitation obtained by other authors

Author	Study Area	$\nabla_z \delta^{18}\text{O}_P$ (‰/km)
This work	Sierra Seca Range	-2.9
Moral Martos (2005)	Sierra de Segura Range	-2.8
Hornero-Díaz (2018)	Chorros de Río Mundo	-4.5
Cruz-San Julián et al. (1992)	Sierra de Segura Range	-5.7
Cruz-San Julián et al. (1992)	Sierra de Cazorla Range	-3.6
Cruz-San Julián et al. (1992)	Sierra de Baza Range	-3.5
Cruz-San Julián et al. (1992)	Sierra de Gádor Range	-3.1
Cruz-San Julián et al. (1992)	Sierra de Lújar Range	-2.8
Vallejos et al. (2015)	Sierra de Gador Range	-1.9
Liñán-Baena (2003)	Sierra de las Nieves Range	-3.0
Andreو et al. (2004)	Sierra de las Nieves Range	-3.0
Yanes & Moral (2022)	Southern Spain	-2.9
Jódar et al. (2016)	Southeastern Pyrenees	-2.2
Giménez et al. (2021)	South Central Pyrenees	-3.0
Díaz-Teijeiro et al. (2009)	Iberian Peninsula	-3.5
Poage and Chamberlain (2001)	Alps	-3.0